Efficiency and cost effectiveness of large-area perovskite-based tandem solar cells

Manoj Jaysankar & Tom Aernouts, imec, Genk, Belgium

Abstract

Tandem solar cells combine several solar cells with different photoabsorbers, stacked in a descending order of bandgap energies. They come in many flavours, but one promising combination is a bottom cell of c-Si or copper indium gallium selenide (CIGS) and a top cell of perovskite. Perovskite solar cells are thin-film solar cells with many advantages, such as a low-cost, high-throughput sheet-to-sheet and roll-to-roll production, and a tuneable bandgap. Their long-term instability, however, is a challenge that needs to be overcome in order to make these cells a success. In this paper it is demonstrated that, by combining comprehensive loss-reduction strategies with effective large-area fabrication, perovskite-based tandem solar modules have the potential to yield power conversion efficiencies (PCEs) that are significantly higher (PCE of up to 45%) than those of established PV technologies, and can be manufactured on an industrial scale.
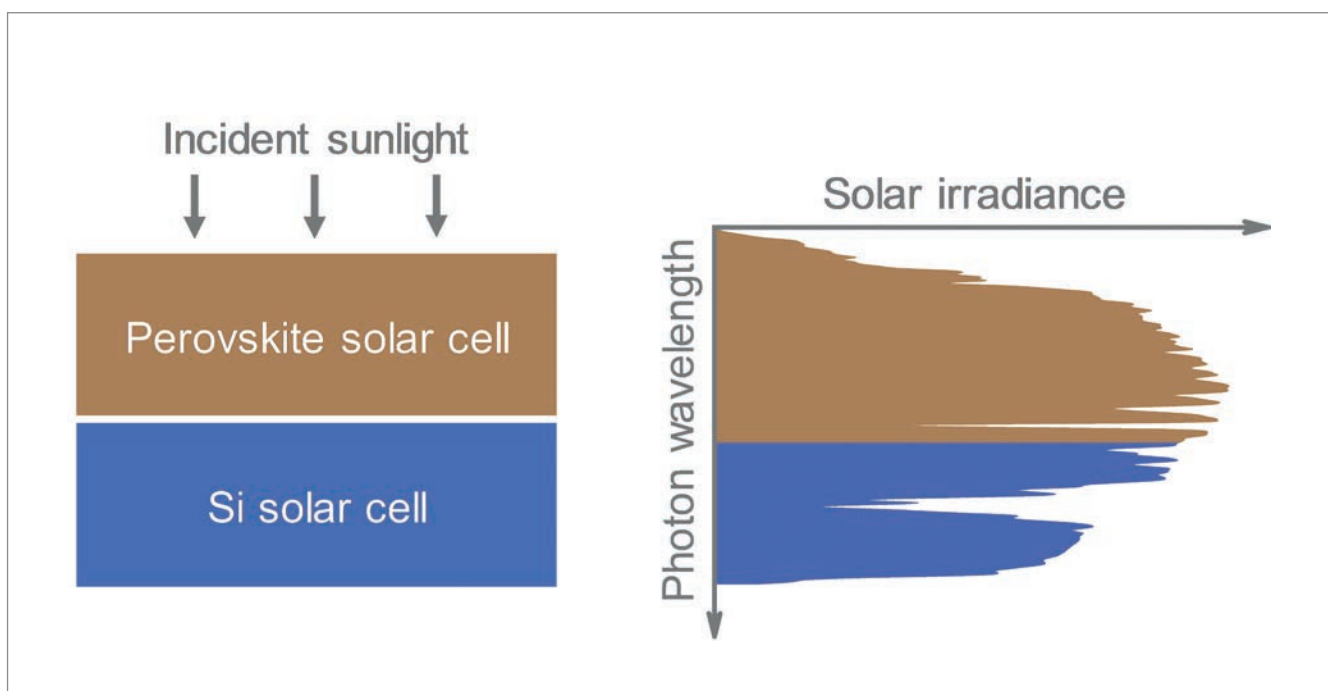
Tandem solar cells

Tandem solar cells comprise several solar cells with different bandgaps coupled with each other, enabling more-efficient harvesting of solar irradiation. In tandem solar cells, cells with different photoabsorbers are stacked in a descending order of bandgap energies (Fig. 1).

Since solar cells with wider-bandgap photoabsorbers generate higher voltages, thermalization losses are significantly reduced in tandem solar cells, compared with single-junction solar cells that absorb the same number of photons; this results in a higher PCE for tandem solar cells.

Tandem solar cells have been widely used for space applications. Such tandem solar cells comprise up to five subcells based on III-V semiconductors, and exhibit PCEs of up to 38.8% under 1 Sun illumination. However, these tandem solar cells have a high degree of complexity and are expensive to manufacture on a large scale. The use of III-V based tandem solar cells is therefore restricted to niche applications, such as powering spacecraft.

For terrestrial applications, manufacturing costs profoundly influence the extent of deployment. Since the terrestrial PV market is dominated by c-Si solar cells, adding a low-cost absorber on top of the c-Si, resulting in high-efficiency tandem solar cells, will be a more promising

Figure 1. Schematic of a tandem solar cell comprising two solar cells with descending bandgap energies. Incident photons with energies above the bandgap of the top solar cell are harvested at a higher voltage by the wider-bandgap top solar cell. The lower-energy (longer-wavelength) photons transmitted by the top solar cell are harvested by the bottom solar cell.

"Thermalization losses are significantly reduced in tandem solar cells."

route to lowering the levelized cost of electricity (LCOE). Until a few years ago, there was a lack of efficient, low-cost solar cells that could be used in a tandem configuration with the PV technologies established in the market. However, the advent of perovskite solar cells and their rapid progress has changed the status quo. Additionally, the feasibility of fabricating perovskite solar cells through solution processing enables low-cost, high-throughput sheet-to-sheet, and in the longer term roll-to-roll, production.

The advantages and challenges of perovskite solar cells

Perovskite, a mineral containing calcium titanate ($CaTiO_3$), was discovered in 1839 and named after the Russian mineralogist Lev Perovski. Today, the term *perovskite* is used to denote all the compounds that have a crystal structure similar to $CaTiO_3$. The generic chemical formula of perovskites is ABX_3, where A and B are positively charged ions of different sizes and X is a negatively charged ion.

Depending on the choices of A, B and X ions, perovskites can be insulators, semiconductors, conductors or superconductors. Perovskites used in solar cells are crystalline semiconductors and are called *hybrid metal halide perovskites*. In such perovskites, the A site is usually occupied by monovalent methylammonium $CH_3NH_3^+$ (MA) or

formamidinium $CH(NH_2)_2^+$ (FA) or caesium (Cs^+), or a combination of these. The B site is taken up by bivalent lead (Pb_2^+) or tin (Sn_2^+), or a mixture of both. The X site is reserved for halides, such as iodide (I^-), bromide (Br^-) or chloride (Cl^-), or a mixture of these.

The most widely researched perovskites for solar cells are lead halide perovskites; they are also the most efficient owing to their remarkable optoelectronic properties. They have a direct optical bandgap, making them promising materials for solar cells as well as for light-emitting diodes and photodetectors. In particular, they offer the following advantages:

- Perovskites have high absorption coefficients of the order of $10^5 cm^{-1}$ in the visible spectral range. Consequently, a perovskite layer of several hundred nanometres is enough to absorb most of the incident light. Besides leading to lower material cost, such thin layers are beneficial for efficient extraction of photo-generated charge carriers.
- Perovskites have sharp absorption edges that translate to low Urbach energies around 15meV, which is comparable to that of gallium arsenide, a direct bandgap crystalline semiconductor of very high optoelectrical quality. The low Urbach energy implies a low degree of structural disorder in the perovskite.

- Perovskites have a very low concentration of deep-level defects. Because of the combination of low Urbach energy and low concentration of

Figure 2. Schematic of the different architectures of perovskite solar cells: (a) mesoporous, (b) planar n-i-p, and (c) planar p-i-n.
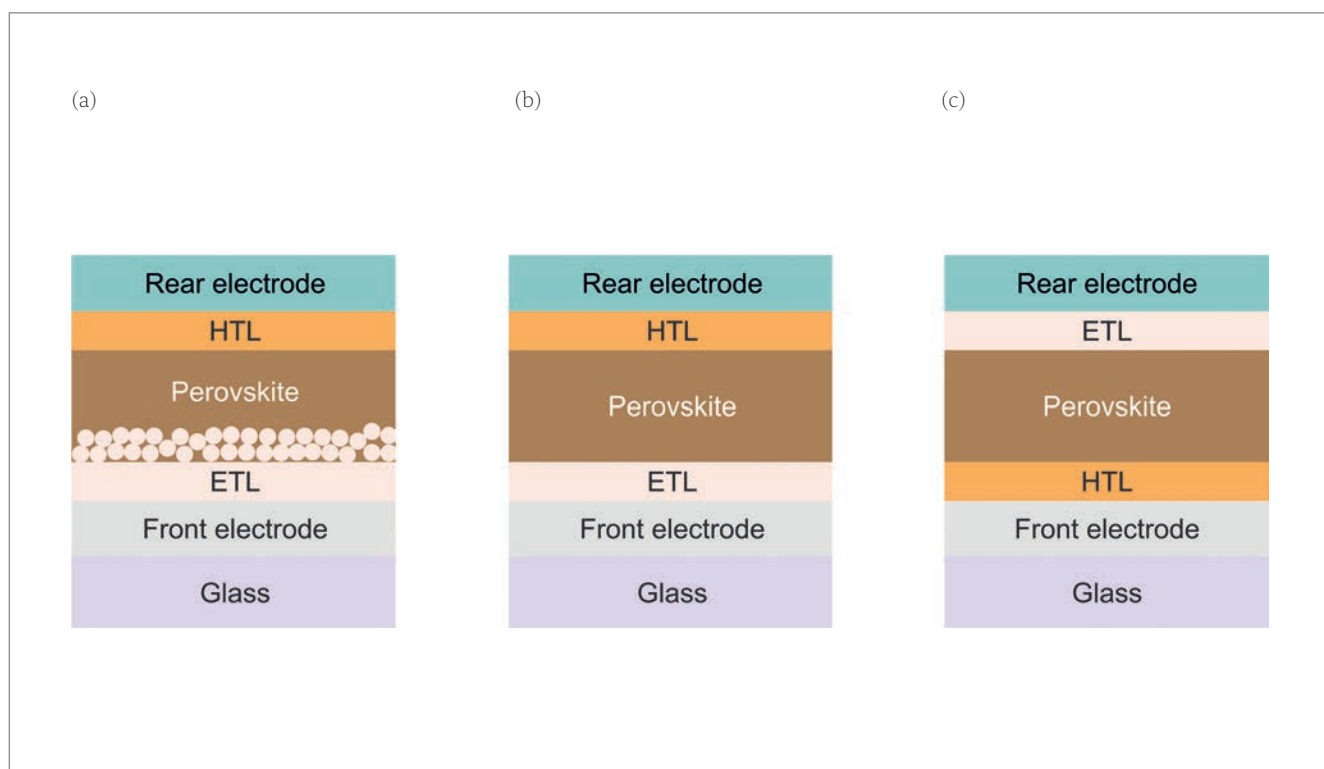
deep-level defects, perovskite solar cells exhibit high open-circuit voltages (V_{oc}) in relation to their bandgap (E_G). The V_{oc} deficit ($E_G - qV_{oc}$) in perovskite solar cells is one of the lowest among all solar cell technologies.

Another noteworthy property of perovskites that makes them attractive for solar cells is the long diffusion length of charge carriers. A charge-carrier diffusion length exceeding 1μm has been demonstrated in polycrystalline perovskite films, while in perovskite single crystal the value is around 175μm. Such long diffusion lengths are made possible by the combined effect of high mobility and long lifetime of charge carriers, primarily because of a low concentration of deep-level trap states in the perovskite. The long charge-carrier diffusion length, coupled with the small thickness of the perovskite layer (thanks to the high absorption coefficient), leads to a high charge-carrier collection efficiency in perovskite solar cells.

Despite the remarkable properties and excellent performance of perovskite solar cells, their prospects of commercialization have been dampened by their long-term instability. However, extensive research into this key aspect has recently resulted in solar cells with improved stability over a period of several thousand hours.

Architecture of the perovskite solar cell

Most perovskite solar cells are fabricated on glass substrates, although fabrication on flexible plastic substrates is also feasible. The primary layers in a typical perovskite solar cell include a *front electrode*, which is usually a transparent conductive oxide (TCO) deposited on the substrate, an *electron transport layer* (ETL), a *photoactive perovskite layer*, a *hole transport layer* (HTL), and a *rear electrode*, which can be a metal or a TCO.

Perovskite solar cells belong to the so-called thin-film photovoltaics (TFPV) and are classified into three categories on the basis of their architecture: mesoporous, planar n-i-p, and planar p-i-n (Fig. 2).

The *mesoporous architecture* is derived from dye-sensitized solar cells, where a mesoporous scaffold is used for better extraction of charge carriers. As perovskite solar cells evolved from dye-sensitized solar cells, the mesoporous architecture was maintained during their early development. The architecture typically uses a mesoporous structure of TiO_2 made of nanoparticles, on top of a compact TiO_2 layer as the ETL. The perovskite is then deposited on the mesoporous scaffold, filling the vacant spaces up to the compact TiO_2 layer. With such a design, the interfacial surface area between the ETL and the perovskite is substantially increased, thus increasing the efficiency of electron extraction. As the understanding of the

> ### "The use of certain mixed cations can remedy the phase segregation of perovskites and thus lead to photostable behaviour."

fundamental properties of perovskites improved, and with the discovery of their ambipolar conductivity and long charge-carrier diffusion lengths, the mesoporous device architecture gave way to the less complex planar architectures.

In the *planar architectures*, the mesoporous scaffold is replaced by a planar ETL. Planar perovskite solar cells come in two flavours: n-i-p and p-i-n. In the case of the n-i-p architecture, the ETL is first deposited on the TCO/glass substrates followed by the perovskite and then the HTL. In n-i-p perovskite solar cells, the *ETL* is in front of the perovskite, facing the incident light, while in p-i-n perovskite solar cells, the *HTL* is in front of the perovskite, facing the incident light. Planar architectures are simpler to fabricate than the mesoporous architecture and allow a wide range of material choices for the transport layers. Although the current record perovskite solar cell with a PCE of 23.3% has a mesoporous architecture, the majority of high-efficiency planar perovskite solar cells, including the ones discussed in this work, use the n-i-p architecture.

A tuneable bandgap

Despite the challenges, high-efficiency perovskite solar cells are currently the most promising low-cost candidates for tandem solar cells with established PV technologies, for terrestrial applications. An interesting property of perovskites, particularly attractive from a tandem perspective, is the ease of bandgap tuneability. The bandgap of most perovskites can be tuned simply by varying their chemical composition, most commonly the anion; the replacement of ions alters the size of the perovskite crystal lattice, thus changing the bandgap. This interesting property enables the fabrication of perovskites with bandgaps ranging from 1.1eV to 3.2eV.

The most commonly used perovskites for high-efficiency solar cells have a bandgap of ~1.6eV. For tandem applications with c-Si and copper indium gallium selenide (CIGS), perovskite bandgaps between 1.7eV and 1.8eV are of particular interest. However, the PCE of such wide-bandgap perovskite (1.7– 1.8eV) solar cells are lower than expected.

One of the reasons for the low performance of wide-bandgap perovskite solar cells is related to their photo-instability. Under continuous illumination, the perovskites tend to phase segregate, leading to degradation; this phenomenon has been shown to occur in certain wide-bandgap perovskites that have mixed halides (I^- and Br^-) as anions. The phase segregation
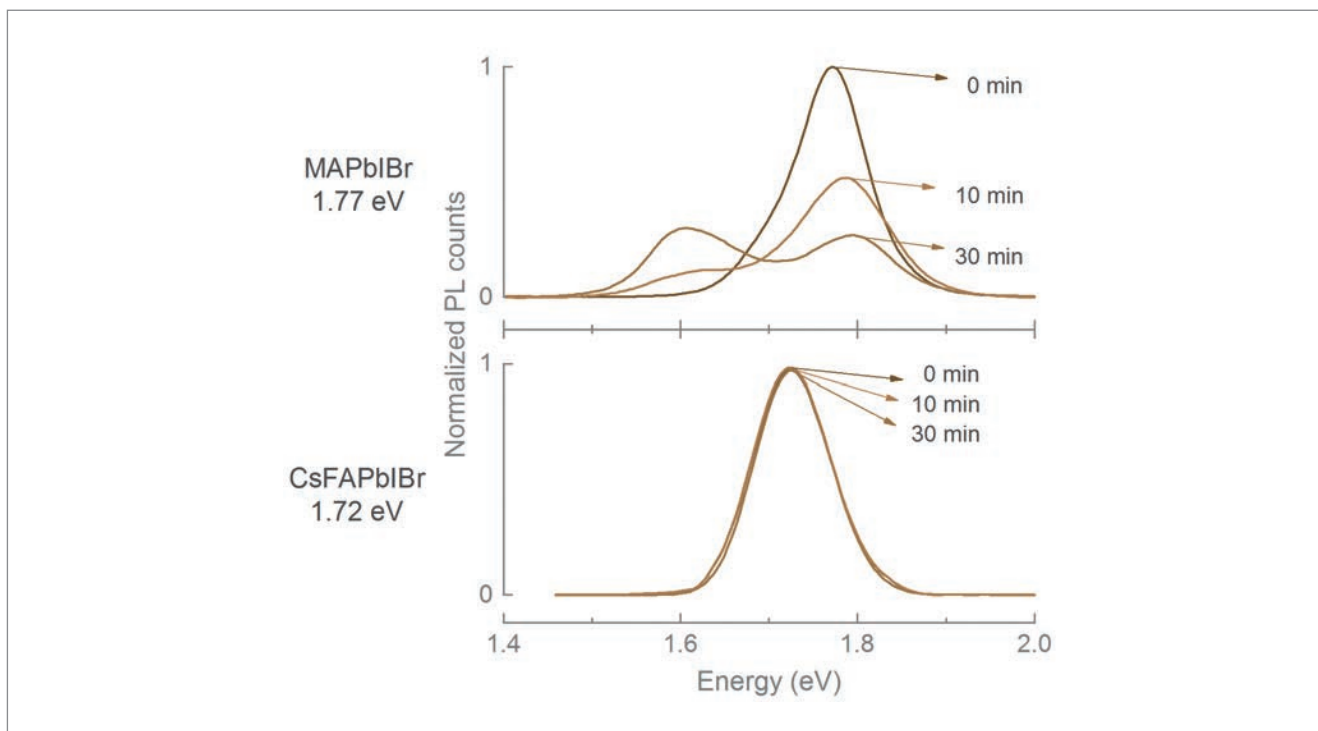
Figure 3. PL spectra of MAPbIBr and CsFAPbIBr thin films under continuous AM1.5G irradiation.

has a significant effect on the performance of such wide-bandgap solar cells, reducing their effectiveness as a top solar cell in tandem solar cells. It has been shown at imec that the use of certain mixed cations can remedy the phase segregation of perovskites and thus lead to photostable behaviour.

How to address the photo-instability of perovskite cells

The photostability of two different mixed-halide perovskites, namely methylammonium lead iodide–bromide, $CH_3NH_3Pb(I_{0.6}Br_{0.4})_3$ (MAPbIBr) with a bandgap of 1.77eV, and caesium formamidinium lead iodide–bromide, $Cs_{0.15}(CH_5N_2)_{0.85}Pb(I_{0.71}Br_{0.29})_3$ (CsFAPbIBr) with a bandgap of 1.72eV, is investigated. The phase stability of both perovskites, light soaked under continuous AM1.5G illumination, was characterized by photoluminescence (PL) measurements.

The PL response of MAPbIBr thin films changes over time, with the PL peak corresponding to the pristine MAPbIBr perovskite phase splitting into two separate peaks over time (Fig. 3). The splitting of the PL peak indicates the segregation of the pristine MAPbIBr perovskite phase into iodide-rich and bromide-rich phases under illumination. The iodide-rich phase (indicated by the PL peak at

~1.6eV) limits the electrical performance, resulting in a reduction in V_{oc} of the MAPbIBr solar cells over time.

On the other hand, CsFAPbIBr mixed-halide perovskite does not exhibit photoinduced phase segregation. The CsFAPbIBr thin films show a similar PL response, with no peak splitting, even after 30 min of light soaking, suggesting that CsFAPbIBr perovskite is phase stable under illumination. Additionally, long-term light stability tests reveal no undue degradation of the 1.72eV CsFAPbIBr solar cells, compared with standard 1.56eV perovskite solar cells. The phase stability is also reflected in a stable V_{oc} of the CsFAPbIBr solar cells over time. Although these solar cells exhibit stable voltage output, their V_{oc} deficit is 0.62V; such a large V_{oc} deficit is unfavourable for tandem applications, considering the low current output of wide-bandgap perovskite solar cells.

Addressing the large V_{oc} deficit in wide-bandgap perovskite cells

Wide-bandgap perovskite solar cells also generate less current than the standard perovskite (1.6eV) solar cells owing to their bandgap. Nevertheless, the lower current is expected to be compensated by a higher voltage output in the wide-bandgap perovskite solar cells. However, the V_{oc} of wide-bandgap perovskite solar cells has so far been lower than expected, with a V_{oc} deficit greater than 0.6eV. Interestingly, the V_{oc} deficit in standard perovskite solar cells is just 0.4eV, and their PCE is considerably higher than with wide-bandgap perovskite solar cells. This has led to

"The constraints on the optimal bandgap of the top and bottom solar cells are more relaxed for the four-terminal configuration."
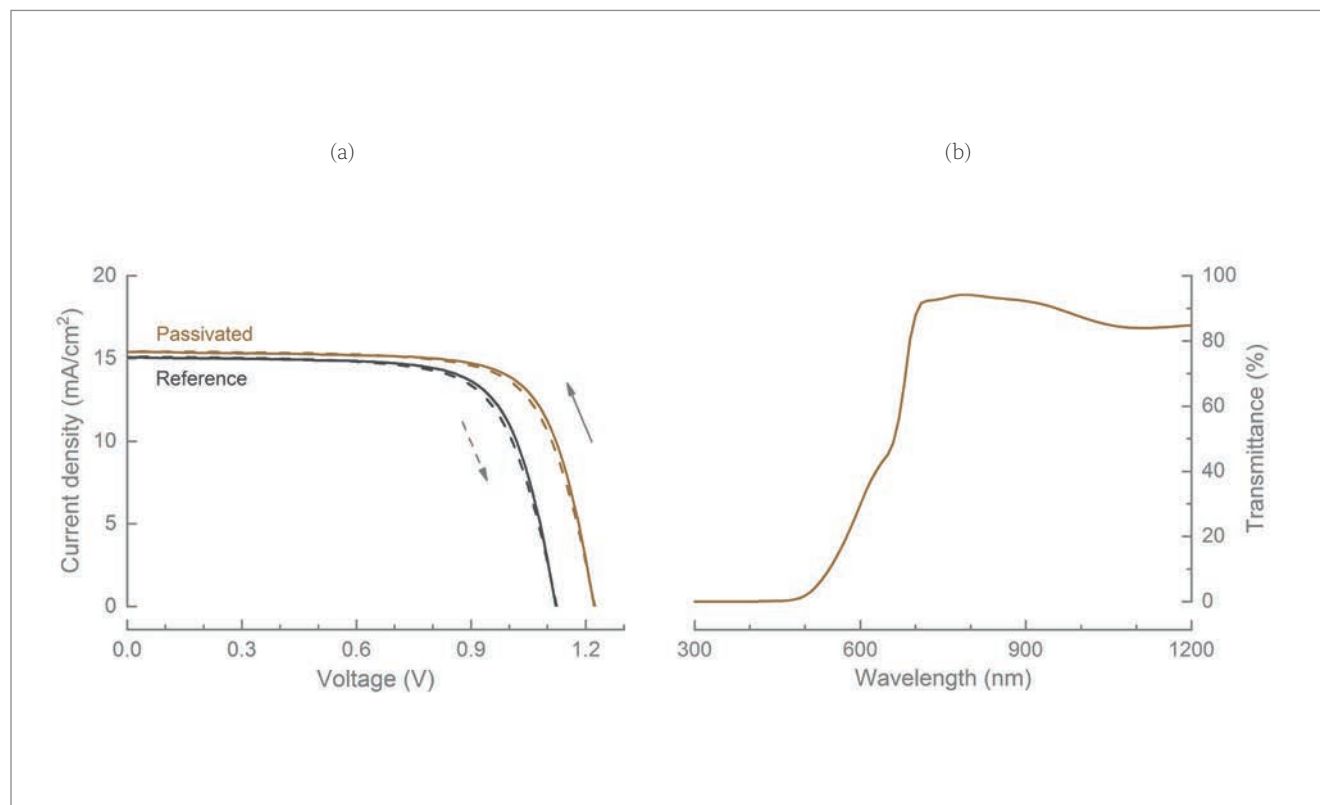
Figure 4. (a) Current density–voltage characteristics of semi-transparent CsFAPbIBr solar cells with interfacial passivation layer ('Passivated') and without ('Reference'), measured in forward and reverse directions. (b) Transmittance spectra of a passivated semi-transparent CsFAPbIBr solar cell.

Device	J_{sc} [mA/cm^2]	V_{oc} [V]	Fill factor [%]	Aperture PCE$_{SPO}$ [%]
Reference CsFAPbIBr	15.1 ± 0.13	1.11 ± 0.03	70.1 ± 0.7	11.7 ± 0.1
Passivated CsFAPbIBr	15.4 ± 0.11	1.22 ± 0.02	73.4 ± 0.4	13.8 ± 0.1
c-Si stand-alone	41.3 ± 0.02	0.691 ± 0.002	80.6 ± 0.1	23.0 ± 0.01
c-Si in tandem	24.1 ± 0.03	0.678 ± 0.002	81.2 ± 0.1	13.3 ± 0.03
CsFAPbIBr–Si tandem				27.1 ± 0.1

Table 1. PV parameters of semi-transparent CsFAPbIBr perovskite and c-Si solar cells, measured under 1,000W/m^2 AM 1.5G irradiance. The reported power conversion efficiency PCE$_{SPO}$ is the stabilized power output of the solar cells tracked at the maximum power point for 10 min

many research groups using standard perovskites for top solar cells in tandem with c-Si and CIGS solar cells, although the bandgap combination is not optimum. Through effective interface passivation, 1.72eV mixed-halide perovskite solar cells with a V_{oc} deficit of just 0.5V have been demonstrated; this is the lowest reported value for a mixed-halide perovskite system with a bandgap wider than 1.7eV (see also Fig. 4(a)).

Better optimization of the cells in the stack

Perovskite-based tandem solar cells are commonly fabricated in two configurations: two-terminal and four-terminal.

In *two-terminal* tandem solar cells, the top solar cell is processed directly on the bottom solar cell, and the two cells are connected in series. This configuration requires only one transparent electrode, and thus has potentially lower parasitic absorption. For efficient operation of two-terminal tandem solar cells, however, the currents generated by the top and bottom solar cells must be similar. As a result, the overall current output of the tandem solar cell will be limited by the lower of the currents generated by the individual subcells. Additionally, seasonal and angular variations in the solar irradiance significantly impact the overall performance of two-terminal tandem solar cells. Consequently, the constraints on the optimal bandgaps of top and bottom solar cells are stricter for the two-terminal configuration. The influence of angular variations of the solar irradiance can be mitigated by employing solar tracker systems, but the use of such systems leads to increased costs.

In the case of *four-terminal* tandem solar cells, the top and bottom cells are electrically isolated from each other, and the output power is extracted separately. This configuration does not

Device	Aperture area [cm^2]	I_{sc} [mA]	J_{sc} [mA/cm^2]	V_{oc} [V]	Fill factor [%]	Aperture PCE$_{SPO}$ [%]
Perovskite	0.13		21.1 ± 0.15	1.07 ± 0.04	72.3 ± 0.9	16.7 ± 0.1
	4	11.1 ± 0.1	19.4 ± 0.1	7.595 ± 0.001	70.1 ± 1.1	14.8 ± 0.1
CIGS	3.8	13.1 ± 0.08		2.692 ± 0.009	75.6 ± 1.0	7.1 ± 0.05
Perovskite–CIGS tandem	0.13					23.8 ± 0.1
	3.8					21.3 ± 0.1

Table 2. PV parameters of semi-transparent perovskite and CIGS solar cells and modules in a four-terminal configuration, measured under 1,000W/m^2 AM1.5G irradiance; the response of CIGS device is measured with the incident light filtered through a semi-transparent perovskite solar module. The reported power conversion efficiency PCE$_{SPO}$ is the stabilized power output tracked at the maximum power point for 10 min. The J_{sc} values reported for the perovskite module are normalized to a single cell, for easier comparison with 0.13cm^2 cells.

require current matching of the two solar cells, and therefore enables independent optimization of the subcells and modular fabrication. For the final assembly, both solar cells are simply mechanically stacked; this configuration requires more than one transparent electrode, leading to increased parasitic absorption. Moreover, on a system level, additional inverters/converters are required to drive the top and bottom solar cells individually, thus increasing the balance-of-system cost. Nevertheless, as a result of the independent power extraction from the top and bottom solar cells, the output of four-terminal multijunction devices is less affected by seasonal and angular variations in solar irradiance, thereby potentially resulting in greater energy yield than for two-terminal tandem solar cells.

Consequently, the constraints on the optimal bandgap of the top and bottom solar cells are more relaxed for the four-terminal configuration, providing additional flexibility in design over the two-terminal configuration. The work reported in this paper focuses on the four-terminal configuration of perovskite-based (perovskite–Si and perovskite–CIGS) tandem solar cells. As discussed above, photostable, wide-bandgap, mixed-halide perovskite solar cells were fabricated, and high V_{oc} was achieved by careful control of the perovskite–HTL interface.

The current–voltage characteristics of reference and passivated CsFAPbIBr solar cells are shown in Fig. 4(a). The passivation significantly improves the V_{oc} and fill factor of the solar cells, boosting the PCE from 11.7% to 13.8%. Furthermore, the CsFAPbIBr solar cells exhibit an average transmittance of 90% in the wavelength range 700–1,200nm (Fig. 4(b)). The high transmittance, coupled with a high V_{oc}, makes the passivated CsFAPbIBr solar cells attractive for highly efficient tandem solar cells.

"By combining comprehensive loss reduction strategies with effective large-area fabrication, perovskite-based tandem solar modules with a PCE surpassing that of established PV technologies can be realized on an industrial scale."

Four-terminal tandem solar cells were then fabricated by combining the passivated CsFAPbIBr solar cells with c-Si solar cells. The wider bandgap of CsFAPbIBr compared with standard 1.56eV perovskites allows additional light to reach the bottom Si solar cell, enabling efficient harvesting of solar irradiation. The resulting CsFAPbIBr–Si tandem solar cells exhibit a PCE of 27.1% – the highest reported for a perovskite-based four-terminal tandem solar cell, exceeding the record PCE of single-junction Si solar cells (Table 1).

The scalability of perovskite-based tandem cells

Besides high efficiency on small sizes, the scalability of such perovskite-based multijunction devices needs to be addressed for commercial viability of this technology. To that end, perovskite–CIGS multijunction solar modules of up to two orders of magnitude larger than the small-area cells were fabricated. The key issue with the fabrication of large-area multijunction solar modules lies with the scalability of the perovskite device.

The losses in aperture PCE when scaling up the semi-transparent perovskite device from 0.13cm^2 cells to 4cm^2 modules were investigated. The design of perovskite modules and the choice of subcell lengths (3mm) are discussed in the authors' earlier work [1]. Three loss factors can be identified:

- *Resistance losses* include the loss in aperture PCE due to sheet resistance of the transparent electrodes and the losses at the interconnections of individual cell stripes in a module.

- *Dead area losses* are a consequence of the monolithic module design, where part of the active material is removed through scribes to allow interconnection of individual cell stripes. Dead area is the difference between aperture area and active area of a module.

- *Inhomogeneity losses* account for the variation in uniformity of the layers deposited on different sizes.

The reduction in aperture PCE of the semi-transparent perovskite device when going from a 0.13cm² cell to a 4cm² module is due to a combined effect of all three loss factors. A SPICE-based analogue electronic-circuit simulator was used to estimate the perovskite efficiency when scaling up from a 0.13cm² cell to a 4cm² mini-module comprising seven subcells, each ~2.9mm long [2]. The estimate indicates that dead area loss accounts for ~58% of the difference in aperture PCE, while resistance loss constitutes ~31%. The perovskite modules have a geometric fill factor of 0.91; in other words, 9% of the module aperture area is dead area, which justifiably makes dead area the major loss factor for aperture PCE when going from 0.13cm² cell to 4cm² module.

The width of individual cell stripes in the perovskite solar module is optimized for the sheet resistance of indium tin oxide (ITO) electrodes, as described in the authors' previous work [1], thus minimizing the resistance loss when scaling up from cell to module. The 0.13cm² perovskite cell and the 4cm² perovskite mini-module were fabricated identically on substrates with the same dimensions; therefore, the loss in aperture PCE due to layer inhomogeneity when going from 0.13cm² cell to 4cm² module accounts for just 11% of the total losses.

An all thin-film perovskite/CIGS multijunction module of similar size was fabricated, yielding an overall PCE that substantially outperformed the single-junction PCE of the CIGS single module. For this, a 3.8cm² aperture area module with PCE of 16.7%, provided by the Center for Solar Energy and Hydrogen Research (ZSW), was later used as the bottom cell. When the perovskite module was placed on top, a PCE of 7.1% was still recorded for the CIGS module. The 4cm² perovskite module had an aperture PCE of 14.8%, bringing the total PCE of the perovskite/CIGS multijunction stack to a remarkable 21.3%, on an overall 3.8cm² aperture area (Table 2).

Outlook

Scalable perovskite solar modules have strong potential for low-cost, high-efficiency tandem photovoltaics. Although the demonstrated tandem module design is scalable to commercial dimensions, various factors affect the aperture PCE of such large-area modules. Resistive losses caused by transparent electrodes can be reduced to a certain extent by using better conductive transparent electrodes, such as hydrogen-doped indium oxide and indium zinc oxide. Losses to aperture PCE due to the dead area formed during patterning of the modules can be minimized by advanced laser patterning, which improves the geometric fill factor.

For industrial-level upscaling, large-area linear coating techniques must be employed for the fabrication of perovskite solar modules. Note

that while scaling up to industrial-scale modules, inhomogeneity will be the key loss factor limiting the aperture PCE of the perovskite solar module, and consequently the aperture PCE of the tandem solar module. Homogeneous, large-area perovskite coating and deposition techniques are therefore essential for maintaining the high aperture PCE on large sizes. By combining comprehensive loss reduction strategies with effective large-area fabrication, perovskite-based tandem solar modules with a PCE surpassing that of established PV technologies can be realized on an industrial scale.

....

References

[1] Jaysankar, M. et al. 2017, "Four-terminal perovskite/silicon multijunction solar modules", *Adv. Energy Mater.,* Vol. 7, p. 1602807 (doi:10.1002/aenm.201602807).

[2] Eidelloth, S., Haase, F. & Brendel, R. 2012, "Simulation tool for equivalent circuit modeling of photovoltaic devices", *IEEE J. Photovolt.,* Vol. 2, pp. 572–579 (doi:10.1109/JPHOTOV.2012.2187774).

....

About the authors

Dr. Manoj Jaysankar holds a Ph.D. in electrical engineering from KU Leuven, Belgium. He is a graduate of the Erasmus Mundus Master in Nanoscience and Nanotechnology programme, for which he specialised in nanoelectronics to earn a joint M.Sc. from KU Leuven and Chalmers University of Technology, Sweden. His research at imec focuses on design and development of high-efficiency, perovskite-based tandem solar cells.

Dr. Tom Aernouts is an R&D manager at imec. He received his M.Sc. in semiconductor physics from KU Leuven in 1998, and his Ph.D. in science in 2006 from the same university. Since 2006 he has been the group leader of imec's thin-film PV group, steering imec's thin-film PV research activities, with an initial infrastructure upgrade in 2009 enabling the processing of devices up to 15cm × 15cm, and a subsequent upgrade in 2018 to extend the device size to 35cm × 35cm.
....

Enquiries

Tom Aernouts
imec
Thor park 8320
B-3600 Genk, Belgium

Tel: +32-16 281689
Email: aernouts@imec.be
Website: www.imec-int.com